

This is the accepted manuscript made available via CHORUS. The article has been published as:

Compressibility as a probe of quantum phase transitions in topological superconductors

David Nozadze and Nandini Trivedi

Phys. Rev. B **93**, 064512 — Published 17 February 2016

DOI: [10.1103/PhysRevB.93.064512](https://doi.org/10.1103/PhysRevB.93.064512)

Compressibility as a probe of quantum phase transitions in topological superconductors

David Nozadze and Nandini Trivedi
*Department of Physics, The Ohio State University,
191 W. Woodruff Avenue, Columbus, OH 43210, USA*
(Dated: January 4, 2016)

While there have been recent reports of zero energy modes in single particle tunneling density of states, their identity as Majorana modes has so far not been unequivocally established. We make predictions for the local compressibility κ_{loc} , tuned by changing the chemical potential μ in a semiconducting nanowire with strong spin-orbit coupling and in a Zeeman field in proximity to a superconductor, which has been proposed as a candidate system for observing Majorana modes. We show that in the center of the wire, the topological phase transition is signaled by a divergence of κ_{loc} as a function of μ , an important diagnostic of the phase transition. We also find that a single strong impurity potential can lead to a local *negative* compressibility at the topological phase transition. The origin of such anomalous behavior can be traced to the formation of Andreev bound states close to topological phase transitions. Measurable by a gate-tunable scanning electron transistor, the compressibility includes contributions from both single particle states and collective modes and is therefore a complimentary probe from scanning tunneling spectroscopy which is sensitive to only the single particle density of states.

PACS numbers: 71.10Pm, 03.67.Lx, 74.45.+c, 74.90.+n

I. INTRODUCTION:

The non-Abelian statistics of Majorana fermions, their role in topological quantum computation, and the possibility of realizing them in condensed matter systems, has attracted considerable attention^{1–5}. Majorana fermions can emerge in systems, such as topological insulator-superconductor interfaces^{6,7}, quantum Hall states with filling factor $5/2$, p -wave superconductors⁸, semiconductor heterostructures^{9,10}, half-metallic ferromagnets^{11,12} and ferromagnetic metallic chains¹³. As shown by Kitaev¹⁴, Majorana fermions can emerge at the ends of 1D spinless p -wave superconducting chain when the chemical potential is in the topological regime.

A realization of the Kitaev chain based on a quantum nanowire made of a semiconductor-superconductor hybrid structure has been proposed^{9,10}. In the presence of Rashba spin-orbit coupling, the parabolic bands for the two spin projections get separated. In addition, a Zeeman field h opens up a gap leading to an effectively spinless 1D system when the chemical potential μ lies in the Zeeman gap. The proximity induced superconductivity with a gap Δ can result in the topological phase^{9,10,15,16}. In this regime, the wire can be realized as a Kitaev chain and should have two Majorana localized zero energy modes at the ends. The nanowire can undergo a quantum phase transition from a topologically trivial superconducting phase to the topological one (or vice versa) by changing the chemical potential or the magnetic field.

There have been recent reports of observations of Majorana fermions in tunneling and the fractional Josephson effect^{16–19}. Ref. 20 has reported significant progress in creating the Majorana states where spatial location of Majoranas are detected using a scanning tunneling microscope. All these experimental observations of the

existence of Majorana fermions *assume* that the system is in the topological phase and attribute the zero energy density of states to the proposed Majorana modes. However, since there could be several other sources for the zero bias anomaly^{21–23}, the existence of Majorana modes has so far not been unequivocally established.

We propose here a definitive method to determine whether or not the nanowire is in the topological or trivial state through measurements of the gate-tuned local compressibility. We further discuss the dramatic changes that occur in the local compressibility as a function of the chemical potential μ in the presence of a potential defect or a weak link.

The paper is in two parts: In part I we discuss the local compressibility in the presence of a weak link and a site defect specifically in the Kitaev model which shows a topological to trivial p -wave superconducting transition at $|\mu| = \mu_c = 2t$, where t is the hopping parameter between neighboring sites in the wire.

In Part II we discuss a microscopic model of a nanowire with spin-orbit coupling in proximity to an s -wave superconductor and investigate its local compressibility response to link and site defects. We analyze in detail a specific cut through the phase diagram that shows two phase transitions upon increasing μ from a trivial p -wave superconductor to a topological p -wave superconductor at $\mu = \mu^-$ and a second one from a topological p -wave superconductor to a trivial superconductor with s - and p -wave pairing at $\mu = \mu^+$. We will see below that the transition at μ^- is captured by the simplified Kitaev model; the transition at μ^+ is qualitatively different.

Our main results are the following:

(1) We find very different behavior of the local compressibility κ_{loc} at the edge of the wire and in the center in a clean wire. While the edge harbors Majorana modes

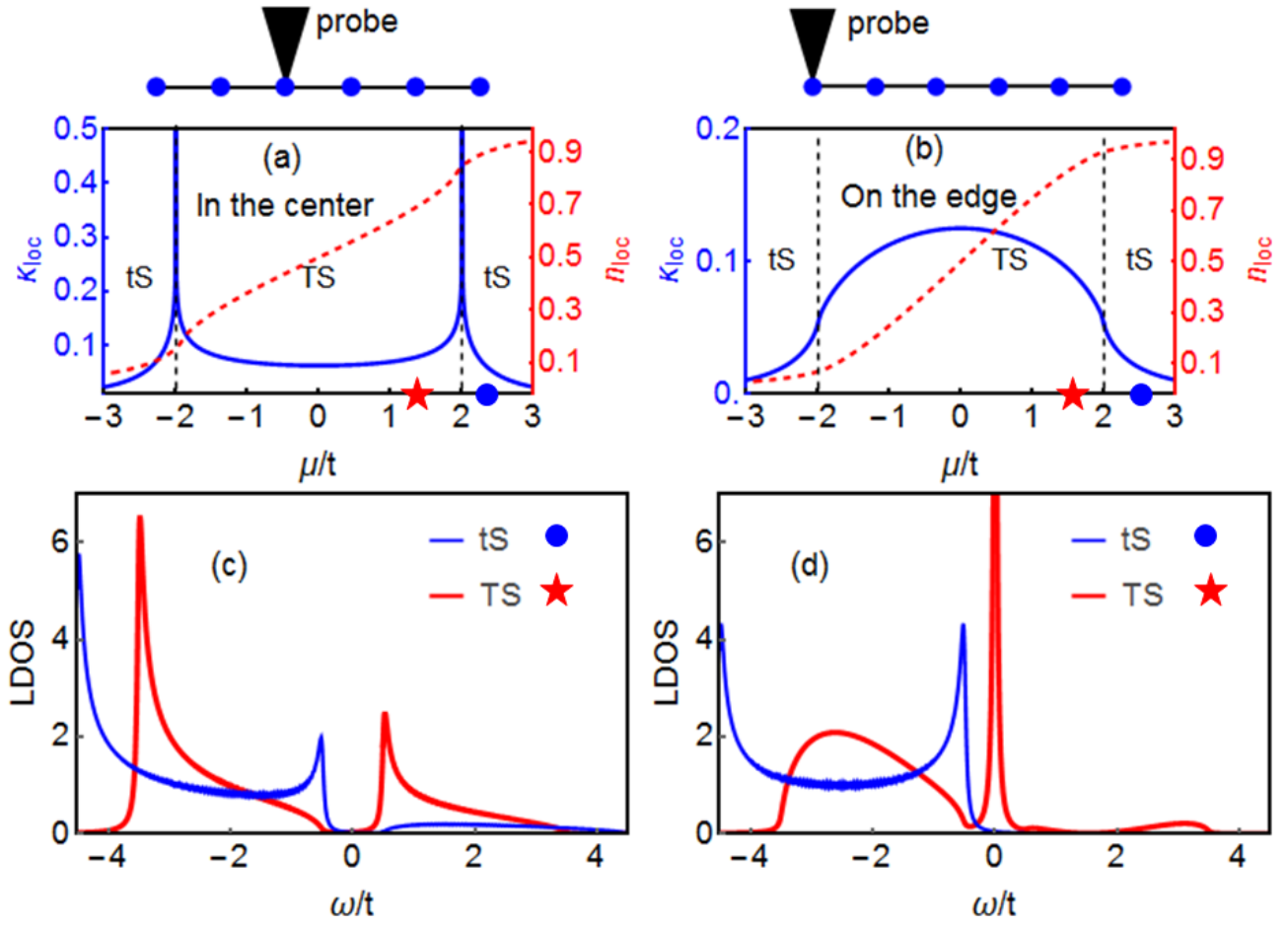


FIG. 1. (Color online). (a) The local particle density n_{loc} (red dashed line) and the local compressibility κ_{loc} (blue solid line) versus chemical potential μ/t in the center of wire for a Kitaev chain with no defects. The compressibility diverges logarithmically at the quantum critical point $\mu = \pm 2t$. The singularity in κ_{loc} is weakened at the edge of the wire (b). (c,d) The local density of states $N_{\text{loc}}(\omega)$ in the trivial ($\mu = 2.1t$, marked by blue circle) and topological ($\mu = 1.5t$, marked by red star) phases. (c) is obtained in the center and (d) at the edge of the wire. Results are presented for chain length $N = 256$ at $T = 0$ with slightly broadened δ -functions in $N_{\text{loc}}(\omega)$.

which show a zero bias anomaly, the density of states in the center is fully gapped. The compressibility on the other hand shows a sharp singularity near the center of the wire at the topological to trivial phase transitions (see Figs. 1, 5), and its behavior at the edge is considerably muted.

(2) A single impurity can dramatically change the local response: a strong impurity leads to the formation of an Andreev bound state (ABS) that remarkably produces a local negative compressibility with a dip at the topological to trivial phase transitions as μ is tuned. An extra peak associated with the bound state appears in κ_{loc} above the transition. For the Kitaev model as well as for the realistic model mentioned above with a transition at μ^- , the ABS is formed in the trivial phase. On the other hand, for the realistic model with the transition at μ^+ , the ABS is formed in the topological phase.

(3) A link impurity with a hopping parameter different in strength but with the same sign as the hopping in the

regular chain, merely suppresses the divergence in κ at the transition for both the Kitaev chain and the realistic model. On the other hand, a link impurity with opposite sign produces zero energy Majorana modes upon fine tuning as discussed below.

Our predictions can be verified by measuring the compressibility as a function of a gate-tunable chemical potential as well as simultaneous measurements of the local density of states using scanning tunneling spectroscopy.

II. KITAEV MODEL WITH DEFECTS

We consider a 1D tight-binding Hamiltonian for spinless fermions with attractive interactions between

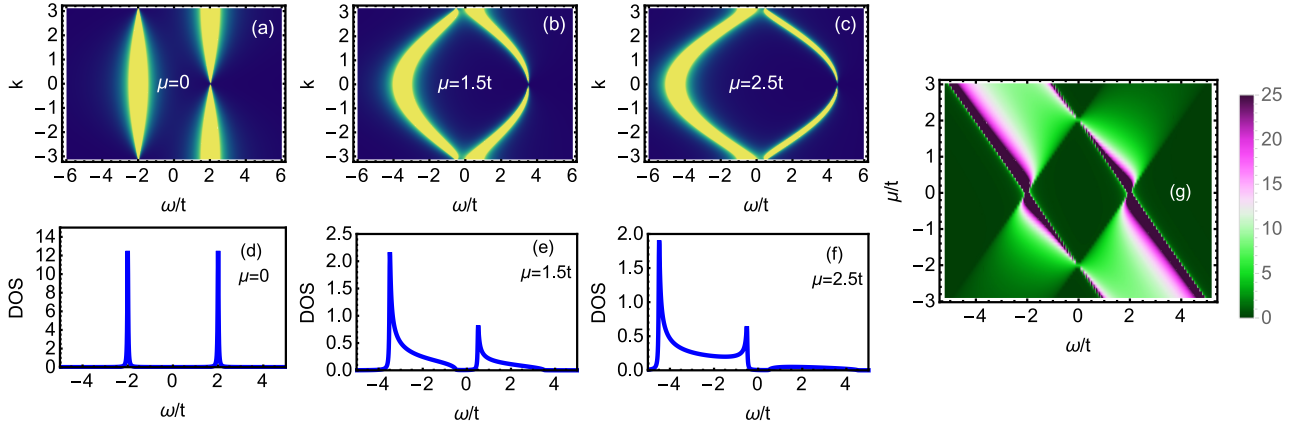


FIG. 2. (Color online). The spectral function $A_k(\omega)$ (intensity encoded in yellow, above a dark blue background which sets the zero) in the topological (a,b) and trivial (c) phases are shown in the upper row with their corresponding density of states $N(\omega)$ in the bottom row for a closed loop. The δ functions in $A_k(\omega)$ and $N(\omega)$ are broadened. At $\mu = 0$, the coherence factors reduce to $|u_k|^2 = (1/2)(1 - \cos(k))$ and $|v_k|^2 = (1/2)(1 + \cos(k))$ which yields a symmetrical $N(\omega) = (1/2)\delta(\omega - 2t) + (1/2)\delta(\omega + 2t)$ around the chemical potential. For $\mu > 0$ there is greater spectral weight for negative energies or “hole-like” states; the opposite is true for negative μ . Panel (g) shows $N(\omega; \mu)$ across the topological phase transition as a function of μ through the closing of the gap and its reopening at $\mu = \pm 2t$.

fermions on nearest neighbor sites:

$$H = -t \sum_i (c_i^\dagger c_{i+1} + \text{h.c.}) - \mu \sum_i c_i^\dagger c_i - \frac{|U|}{2} \sum_i c_i^\dagger c_i c_{i+1}^\dagger c_{i+1}, \quad (1)$$

where c_i^\dagger (c_i) is the creation (destruction) operator for an electron on a site i , t is the near-neighbor hopping parameter, μ is the chemical potential, and $|U|$ is the pairing interaction. If we approximate the interaction term using a p -wave mean field gap function, defined by

$$\Delta_i = |U| \langle c_i^\dagger c_{i+1}^\dagger \rangle, \quad (2)$$

we obtain the Kitaev 1D spinless tight-binding Hamiltonian with p -wave superconducting pairing¹⁴.

In this paper, we consider the effect of defects which we model as on-site impurity potentials V_i or weak links t_i between nearest neighbor sites $(i, i+1)$,

$$H = \sum_i (V_i - \mu) c_i^\dagger c_i - \sum_i t_i (c_i^\dagger c_{i+1} + \text{h.c.}) - \sum_i \Delta_i (c_i^\dagger c_{i+1}^\dagger + \text{h.c.}). \quad (3)$$

In the clean limit, $t_i = t$, $\Delta_i = \Delta$ and $V_i = 0$, and the system reduces to the 1D Kitaev chain¹⁴.

A. Bogoliubov-de Gennes (BdG) approach

We go beyond T -matrix by using the inhomogeneous Bogoliubov-de Gennes (BdG) method to study the effects

of link defects and on-site impurities that is able to capture the inhomogeneous variation of the order parameter around the defect. From the information about the eigenvalues and eigenfunctions, we calculate the local density of states and the local compressibility as discussed below. Even though this is a one-dimensional problem we are justified in ignoring the quantum fluctuations, primarily because we envisage the system as proximity coupled to a bulk superconductor which damps out the fluctuations.

We diagonalize Eq. (3) by defining the operator $\gamma_i = \sum_n (c_n u_n(i) - c_n^\dagger v_n^*(i))$ that leads to BdG equations

$$\begin{pmatrix} h_0 & -\Delta^\dagger \\ \Delta & -h_0 \end{pmatrix} \begin{pmatrix} u_n(j) \\ v_n(j) \end{pmatrix} = E_n \begin{pmatrix} u_n(j) \\ v_n(j) \end{pmatrix}, \quad (4)$$

where the excitation eigenvalues $E_n \geq 0$. $h_0 u_n(i) = (-\mu_i + V_i) u_n(i) - t_i (u_n(i+1) + u_n(i-1))$ and $\Delta u_n(i) = \Delta_i u_n(i+1) + \Delta_{i-1} u_n(i-1)$. The self-consistency condition is given by

$$\Delta_i = U \sum_{E_n > 0} u_n(i) v_n(i+1) \tanh(E_n/2T). \quad (5)$$

The density of particles on site i is

$$n_i = \langle c_i^\dagger c_i \rangle = \sum_n [|u_n(i)|^2 f(E_n) + |v_n(i)|^2 (1 - f(E_n))] , \quad (6)$$

where $f(E_n)$ is the Fermi function. The local single-particle density of states (LDOS) is given by

$$N_i(\omega) = \sum_n [|u_n(i)|^2 \delta(\omega - E_n) + |v_n(i)|^2 \delta(\omega + E_n)] . \quad (7)$$

Here ω is measured relative to the chemical potential μ .

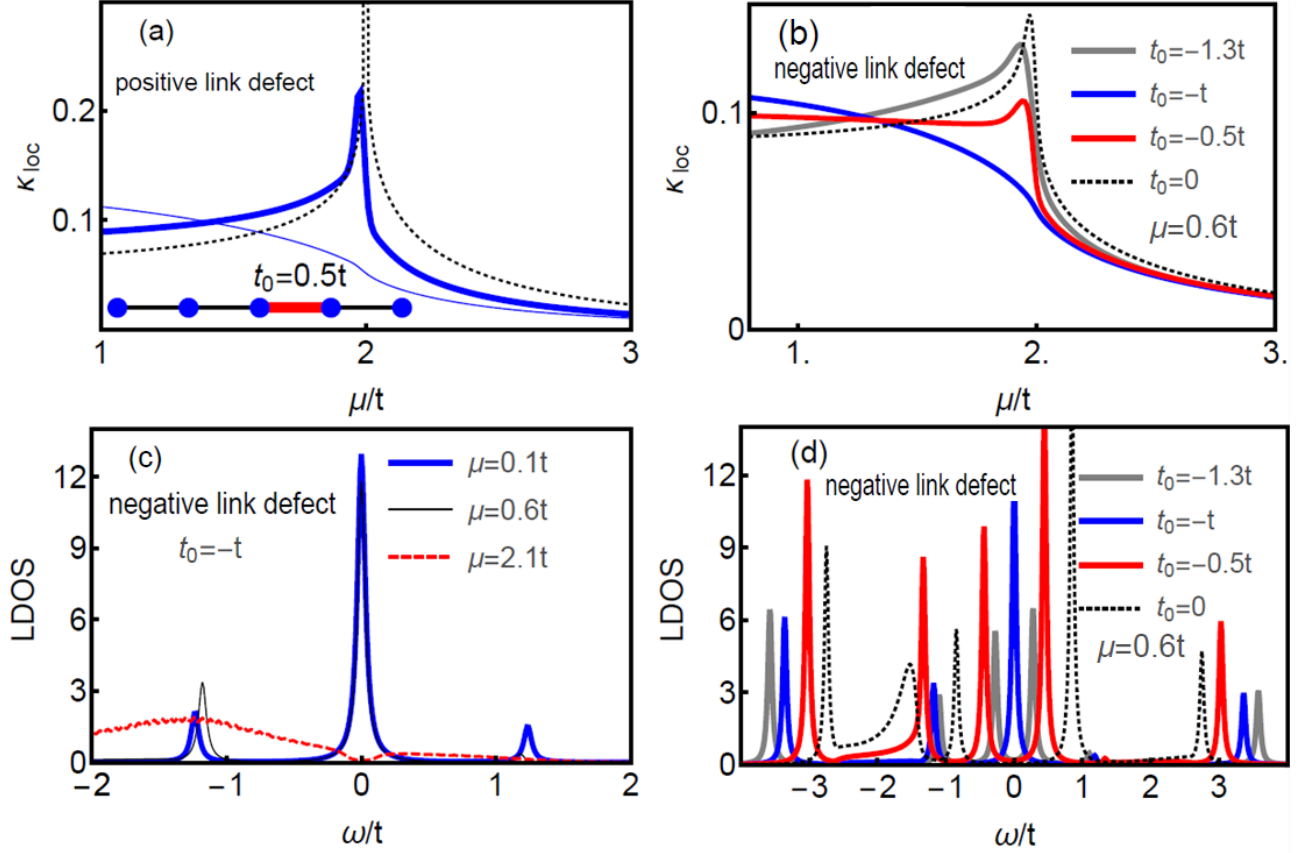


FIG. 3. (Color online). Panels (a,b) The local compressibility κ_{loc} as a function of the chemical potential μ/t for a link defect measured on either side of the link. The link defect is characterized by a hopping parameter $t_0 \neq t$ different from the reference value. Panel (a): Three cases – (i) No defect $t_0 = t$ (black dotted line); (ii) positive link defect with same sign hopping as the reference but with $t_0 = 0.3t$ (blue thick solid line); (iii) cut wire with $t_0 = 0$ (blue thin line). The singularity in κ_{loc} at the topological phase transitions at $\mu = \mu^\pm$ is weakened in the presence of a positive link defect. Panel (b): Negative link defect for several values of the hopping parameter t_0 at $\mu = 0.6t$. (c) Local density of states (LDOS) for a negative link defect showing a bound state (Majorana) at zero energy in the topological phase $\mu = 0.1t, 0.6t$ (blue) and away from zero in the trivial phase $\mu = 2.1t$ (red). In all panels, $\Delta_0 = 1.0t$. (d) $t = -t_0$ corresponds to the majorana state in the topological phase ($\mu = 0.6t$) and others are resonances corresponding to the Andreev bound states.

III. RESULTS: CLEAN KITAEV MODEL

For a clean wire with periodic boundary conditions, i.e. a loop, the Hamiltonian in Eq. (3) can be diagonalized to give $H = \sum_k E_k \gamma_k^\dagger \gamma_k$ using the Bogoliubov transformation $\gamma_k = u_k c_k + v_k c_{-k}^\dagger$ with $|u_k|^2 = 1/2 (1 + \epsilon_k/E_k)$ and $|v_k|^2 = 1 - |u_k|^2$. The quasiparticle excitation energy is given by $E_k = \sqrt{\epsilon_k^2 + |\Delta_k|^2}$ where $\Delta_k = 2it \sin(k)$ and $\epsilon_k = -\mu - 2t \cos(k)$.

A. Compressibility at the topological phase transition

From the number equation at temperature T for the total number of particles N , we have

$$N = \frac{1}{2} \sum_k \left(1 - \frac{\epsilon_k}{E_k} \tanh(E_k/2T) \right). \quad (8)$$

We obtain the isothermal compressibility at finite temperature $\kappa(T) = \left(\frac{\partial N}{\partial \mu} \right)_{T,V}$ to be

$$\kappa(T) = \sum_k \frac{|\Delta_k|^2}{2E_k^3} \tanh(E_k/2T) + \sum_k Y_k \frac{\epsilon_k^2}{E_k^2}, \quad (9)$$

where $Y_k = 1/4T \text{sech}^2(E_k/2T)$ is the Yoshida function.

The low temperature compressibility diverges logarithmically at the quantum critical point $\kappa \sim \log(1/|\mu| - 2t) + T$ as shown in Fig. 1(a). For an open wire, the behavior of κ in the center of the wire, far from the edges, is essentially captured by Eq. (9) that was derived for a closed loop. At $T = 0$ the divergence occurs at $\mu_c = \pm 2t$ caused by the gap in the topological phase $|\mu| < 2t$ closing at the topological phase transition¹⁴ and reopening again in the trivial phase $|\mu| > 2t$. At $T=0$ and for fixed μ , deep in the topological phase ($|\mu| \ll 2t$), $\kappa \sim \Delta^2/t^3$ for $t \gg \Delta$ whereas $\kappa \sim 1/\Delta$ for $t \geq \Delta$.

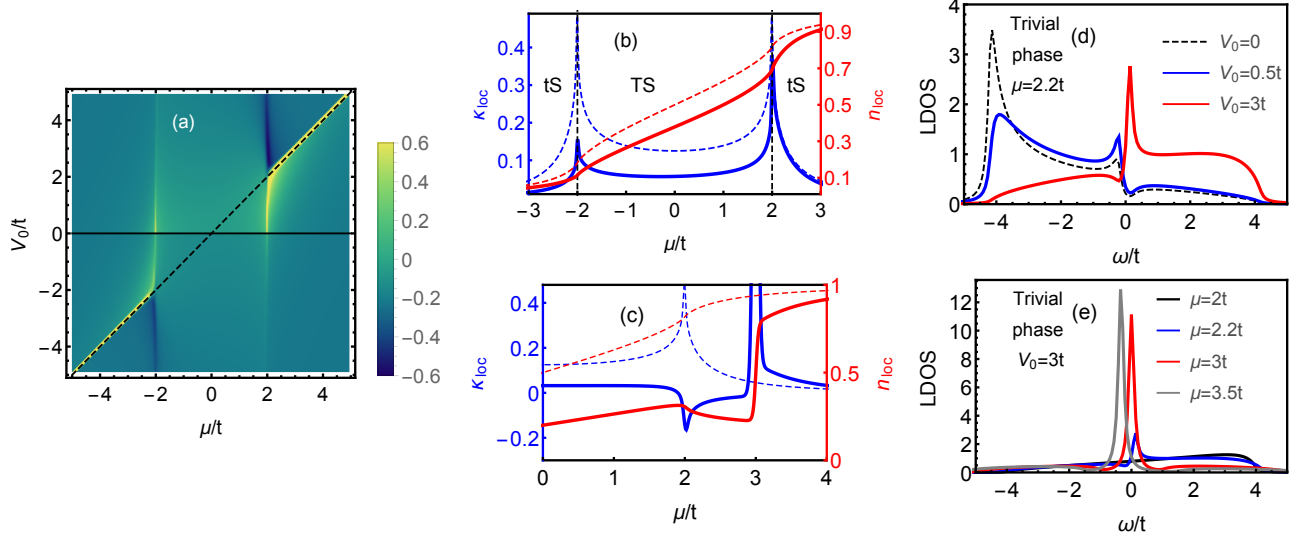


FIG. 4. (Color online). (a) Density plot of κ_{loc} in the $\mu/t - V_0/t$ plane. (b) The local particle density n_{loc} (red) and κ_{loc} (blue) for a local potential defect $V_0 = t < \mu_c = 2t$ (solid) and for the clean system $V_0 = 0$ (dotted). (c) Same as (b) but for a stronger potential defect $V_0 = 3t > \mu_c = 2t$ (solid) compared to the clean case (dotted). Close to the topological phase transition $\mu \approx \mu_c$, κ_{loc} becomes negative and an extra peak appears in the trivial phase. (d) Local density of states (LDOS) in the trivial superconductor for various values of V_0 and $\mu = 2.2t$. (e) LDOS in the trivial superconductor for a fixed $V_0 = 3t$ and for various values of μ . For $\mu = V_0$ there is a zero-energy bound state but this is not a Majorana mode (see text).

To obtain κ at the edge of the wire, we have to solve the inhomogeneous problem using the BdG method as described in section II.A and specifically from Eq. (6). We obtain the local compressibility $\kappa_{\text{loc}} \equiv \kappa_i = \partial n_i / \partial \mu$ by differentiating the local density with respect to the *global* chemical potential μ . We see from Fig. 1(c) that the singularity in κ at μ_c is completely suppressed at the edge of the wire.

B. Single particle density of states

It is useful to contrast the behavior of the compressibility κ from the single particle density of states (DOS). The spectral function $A_k(\omega) = |u_k|^2 \delta(E_k - \omega) + |v_k|^2 \delta(E_k + \omega)$ and DOS $N(\omega) = \sum_k A_k(\omega)$. On the other hand, κ captures both the contributions from the single particles as well as pairs.

As seen in Fig. 2, the DOS shows a gap in both the topological and the trivial phases except at the transition. However, κ is non-zero everywhere because of the contribution from the pairs. Once again for an open wire, the local density of states (LDOS) in the center of the wire essentially reflects the behavior of the closed loop as shown in Fig. 1(c) where both the topological and trivial phases have a finite gap that closes only at μ_c . However, at the edge while the trivial superconductor continues to remain gapped, there are zero energy Majorana modes in the topological superconductor, as is well known from Kitaev's solution.

All the results presented in the figures are at zero temperature and can easily be generalized to finite tempera-

tures from Eqs. (6,7).

IV. RESULTS: KITAEV MODEL WITH DEFECTS

A. Weak link

In the presence of a “positive” weak link, i.e., a link with a hopping parameter that is only different in magnitude but of the same sign as the regular hopping in the wire, the divergence of the local compressibility at the transition $\mu = \pm \mu_c$ is suppressed as shown in Fig. 3 (a). A “negative” link defect with the opposite sign of the hopping parameter has a dramatic effect; for $t_0 = -t$ a Majorana bound state is formed at the two ends of the link. For all values of t_0 there are multiple resonances that should be detectable by a scan probe.

B. Local potential

In the presence of an on-site impurity V_0 , there are several interesting features in the behavior of the local particle density and compressibility as summarized in the density plot of the local compressibility κ_{loc} in the $V_0 - \mu$ plane (see Fig. 4 (a)).

(1) Upon comparing with the results for the clean system, we see that for a repulsive potential $V_0 > 0$, the local density n_{loc} , which is obtained by integrating $N_i(\omega)$ up to zero, is reduced for all μ (Fig. 4 (b,c)), as expected. This

occurs because spectral weight shifts above the Fermi level in the presence of a repulsive potential, as depicted in Fig. 4 (d) for one particular value of μ .

(2) The behavior of local compressibility κ_{loc} and density n_{loc} are remarkably different for $V_0 < \mu_c$ and for $V_0 > \mu_c$. In the former case, while the divergences in κ for the clean problem are cut-off in the presence of the impurity, singularities in the local κ_{loc} nevertheless survive at $\mu = \pm\mu_c$. These singularities are of *unequal* strengths as seen in Fig. 4 (b) for small impurity potential $|V_1| < \mu_c$. This can be understood from the changes to the local density of states by the presence of the impurity. While the states for both $\mu = +\mu_c$ and for $\mu = -\mu_c$ are shifted to positive energies, there is a marked difference in the spectra. In particular, the local density of states for $\mu = -\mu_c$ shows a sharpening and the possible formation of a bound state.

(3) For larger impurity strengths $V_0 > \mu_c$, the effect is quite non-trivial. The local particle density is found to *decrease* around the topological phase transition even as μ increases. Correspondingly, the local compressibility κ_{loc} becomes negative and shows a dip at the transition (Fig. 4 (b)). The reason for the decrease of the local density and the corresponding negative local compressibility is tied to the formation of an Andreev bound state (ABS) around the impurity that starts to form above zero energy close to the topological phase transition.

(4) The bound state formation is induced by the sign change of the order parameter in this unconventional superconductor. As seen in Fig. 4 (b), for a small superconducting gap, the bound state is at a finite energy and is broadened into a resonance. For a fixed V_0 as μ increases, the gap increases and the bound state becomes sharper and moves to zero energy at $\mu = V_0$ (Fig. 4 (e)). At this point the zero energy bound state is detectable as an additional peak in κ_{loc} .

(5) For a negative impurity potential, the ABS forms below the Fermi level and more states shift below the Fermi energy to enhance the local density for all μ . In contrast to the scenario of the positive impurity potential, the ABS does contribute to the local particle density for a negative impurity. As the result, the local particle density starts to increase as μ decreases, until a sharp ABS is formed. This once again causes the local compressibility to become negative around the topological phase transition.

V. REALISTIC MODEL FOR MAJORANA FERMIONS

Turning now to part II of the paper, we consider a more realistic model of a one-dimensional wire with spin-orbit coupling in proximity to a bulk s-wave superconductor. As has been discussed previously in the literature, this system can be described by the Hamiltonian:

$$H = - \sum_{i,\sigma} (\mu - V_i) c_{i\sigma}^\dagger c_{i\sigma} - \sum_{i\sigma} t_i (c_{i\sigma}^\dagger c_{i+1\sigma} + \text{h.c.}) + H_{\text{SO}} + H_Z + H_{\text{Int}}, \quad (10)$$

where c_i^\dagger (c_i) is the creation (destruction) operator for an electron on a site i , t_i the nearest-neighbor hopping and μ is the chemical potential. The spin-orbit coupling and the Zeeman field terms are given by $H_{\text{SO}} = \frac{1}{2} \sum_{i\sigma} \alpha_i [c_{i+1\sigma}^\dagger (i\sigma_y)_{\sigma\sigma'} c_{i\sigma'} + \text{h.c.}]$ and $H_Z = -h \sum_{i\sigma} c_{i+1\sigma}^\dagger (\sigma_z)_{\sigma\sigma'} c_{i\sigma'}$, respectively. Parameters α_i refer to the Rashba spin-orbit coupling and h to the Zeeman field. V_i is the on-site impurity potential. The interaction term $H_{\text{Int}} = -|U| \sum_i c_{i\uparrow}^\dagger c_{i\uparrow} c_{i\downarrow}^\dagger c_{i\downarrow}$, where U is the pairing interaction. In the clean limit $\alpha_i = \alpha$, $t_i = t$ and $V_i = 0$.

We solve the model in Eq. (10) within the Bogoliubov-de Gennes (BdG) self-consistent approach and calculate the local particle density n_{loc} and the local density of states $N_{\text{loc}}(\omega)$ as discussed in section II in Eqs. (6,7).

As shown in Ref. 24, the model in Eq. (10) has several different phases: trivial superconducting phase (tS), topological superconducting phase (TS) with Majorana fermions at ends of chain, Fulde-Ferrell-Larkin-Ovchinnikov phase (FFLO) with spatially oscillating order parameter Δ and non-zero magnetization, insulator phase (INS) with finite energy gap and normal gas (NG) phase without pairing and energy gap (see Fig. 6 (b)). We are interested in a particular slice of the phase diagram in order to investigate the behavior of the compressibility across the topological to trivial phase transitions. We consider the Zeeman field $h = 1.35t$ and spin-orbit coupling $\alpha = t$ that shows two transitions from the topological to the trivial phases as a function of the chemical potential μ at μ^- and μ^+ . We find the quasiparticle excitation energy $E_\pm^2(k) = \epsilon_k^2 + \alpha^2 \sin^2(k) + h^2 + \Delta^2 \pm 2\sqrt{h^2(\epsilon_k^2 + \Delta^2) + \alpha^2 \sin^2(k)}\epsilon_k^2$, where $\epsilon_k = -2t \cos(k) - \mu$. When $h > 0$, the gap ($E_- = 0$) closes at $|\mu^\pm| = (2t \pm \sqrt{h^2 - \Delta^2})$, which corresponds to the phase transitions. The system is in the topological phase when $\mu^- < |\mu| < \mu^+$ and in the trivial phase for $\mu < -\mu^+$ or $\mu > \mu^+$ (see Fig. 6 (c)). For the parameters chosen, $\mu^- \approx 0.84t$ and $\mu^+ \approx 3t$. It is important to note that the system is effectively a “spinless” p -wave superconductor so long as the chemical potential crosses only a single band and the transitions are from the topological phase to a trivial p -wave phase. Once both bands are crossed, the trivial phase has contributions from both s (inter-band) and p -wave (intra-band) pairing channels⁵.

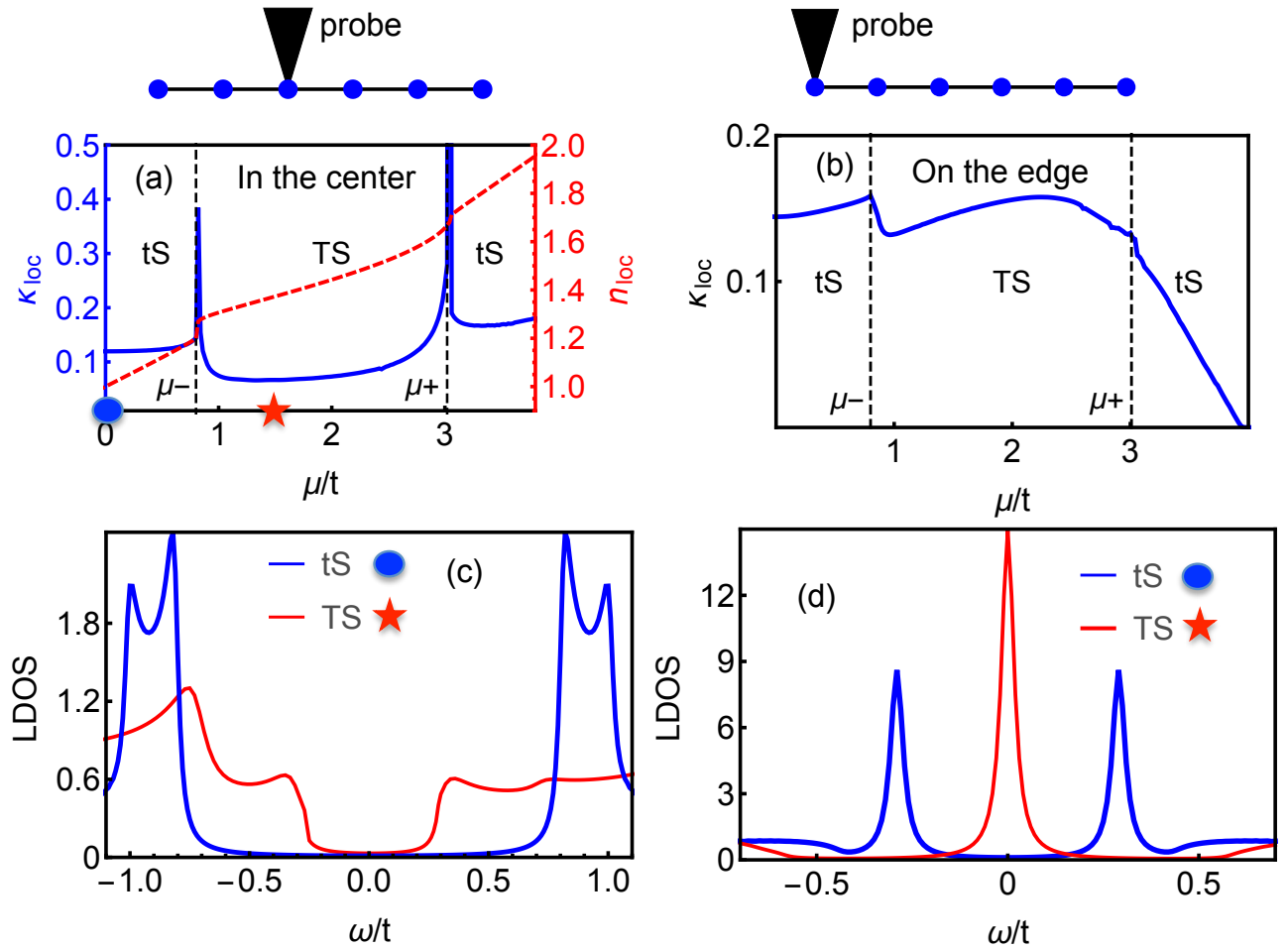


FIG. 5. (Color online). (a) The local particle density n_{loc} (dashed line) and the local compressibility κ_{loc} (solid line) versus chemical potential μ/t in the center of wire. The compressibility has sharp peaks at the transition between trivial (tS) and topological (TS) superconducting phases. The singularity in κ_{loc} is weakened at the edge of the wire (b). (c,d) The local density of states $N_{\text{loc}}(\omega)$, measured relative to the chemical potential μ , in the trivial ($\mu = 0$, blue circle) and topological ($\mu = 1.5t$, red star) phases. Results presented for chain length $N = 256$ at $T = 0$ with slightly broadened δ -functions in $N_{\text{loc}}(\omega)$.

A. Compressibility at the topological phase transition

Similar to the discussion of the Kitaev chain, from the self consistent BdG solutions of Eq. (10), we obtain the local particle number n_{loc} and its dependence on the global chemical potential μ yields the local compressibility $\kappa_{\text{loc}} = \partial n_{\text{loc}} / \partial \mu$. We find that in the center of the wire the local compressibility shows a logarithmic divergence arising from the gap closing linearly between the topological to the trivial phase transitions (Fig. 5 (a)). In contrast, the singularities are weakened on the edge of the wire (Fig. 5 (b)). It is useful to contrast the compressibility which captures the single particle and the pair (collective modes) density of states (DOS), from the behavior of the single particle density of states $N_{\text{loc}}(\omega)$. As seen in Fig. 5 (c,d), the DOS shows a gap in both the topological and the trivial phases except at the transition where the gap gets closed. However, the compressibility

is non-zero in spite of a single-particle gap because of the contribution from the pairs, as was also the case for the Kitaev chain.

This is one of our central results. It highlights the fact that by measuring both the local tunneling DOS at the edge of the wire *and* the local compressibility at the center of the wire as a function of μ it is possible to unequivocally determine when the wire is in the topological phase with Majorana modes localized at the edges. As a control, μ can be varied to bring the wire into a trivial phase with a finite compressibility and a gapped single particle DOS.

We next discuss the effect of a weak link and a single potential disorder on the local compressibility. We show that it is necessary to distinguish the transition from the trivial superconductor (tS) with an order parameter with p-symmetry to a topological superconductor (TS) occurring at μ^- from the one occurring at μ^+ from the TS to tS but with order parameters with both s- and p-

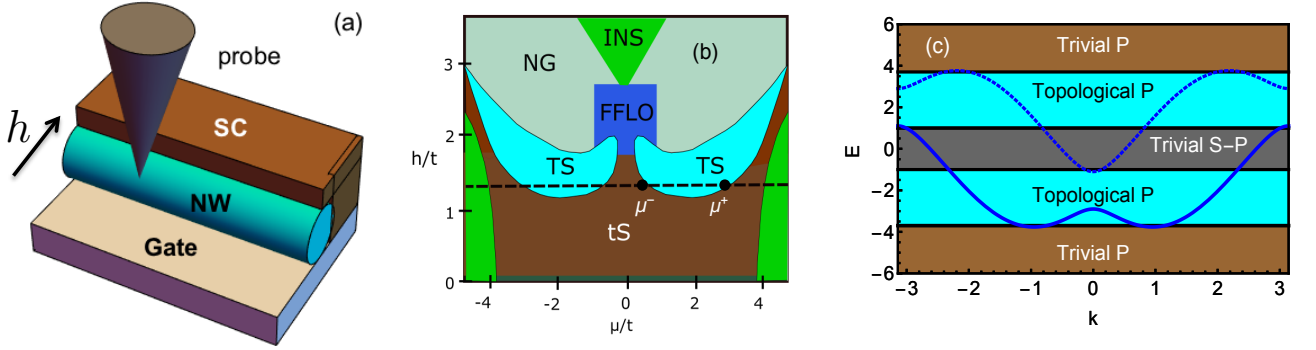


FIG. 6. (Color online). (a) Proposal for measuring local compressibility using an SET (single electron transistor) in the suggested set-up^{9,10} of a nanowire (NW) with spin-orbit coupling in proximity to a superconductor (SC) with an applied magnetic field. (b) Phase diagram of 1D spin-orbit coupled superconductor as function of Zeeman field h/t and the chemical potential μ/t 24. Five different phases can be identified: trivial superconducting (tS), topological superconducting (TS), FFLO, normal gas (NG) and insulator phase (INS). (c) The band structure for a wire with spin-orbit coupling in a magnetic field. As attraction is turned on, different pairing symmetries emerge depending on the location of μ (the Bogoliubov bands have not been shown). Within the first band, the system is described by the Kitaev model that captures the transition from the trivial p to topological p -wave SC. Once the second band is crossed, both interband s -wave and intraband p -wave channels become operative.

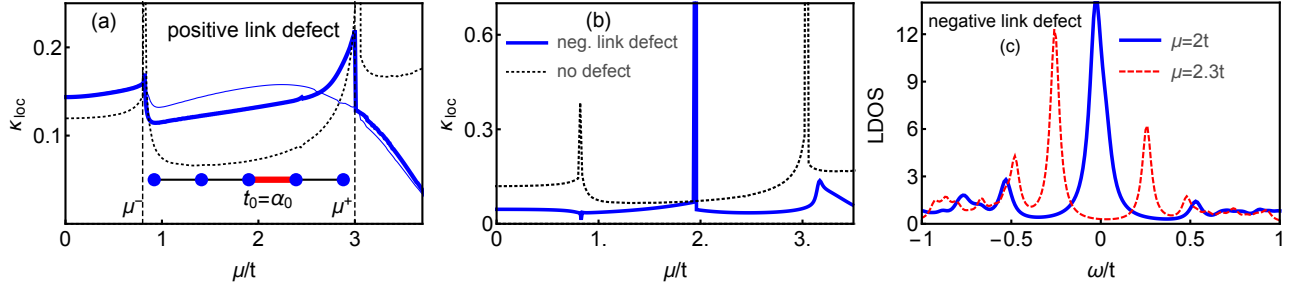


FIG. 7. (Color online). Panels (a,b) The local compressibility κ_{loc} as a function of the chemical potential μ/t for link defects measured on either side of the link. Panel (a) Positive link defect (spin-orbit coupling $\alpha_0 \neq \alpha$ and hopping parameter $t_0 \neq t$ different from the reference values shown for three cases (i) No defect (black dotted line); (ii) $\alpha_0 = t_0 = 0.3t$ (blue thick solid line); (iii) cut wire with $\alpha_0 = t_0 = 0$ (blue thin line). The singularity in κ_{loc} at the topological phase transitions at $\mu = \mu^\pm$ is weakened in the presence of the link defect. Panel (b) Negative link defect with $t_0 = -t$ (blue solid line). The sharp peak in κ_{loc} within the topological phase arises because of the formation of a zero-energy bound state on either side of the link defect. (c) Local density of states (LDOS) for a negative link defect showing a bound state at zero energy at $\mu = 2t$ (blue) and away from zero $\mu = 2.3t$ (red).

symmetry.

B. Weak link

In the presence of a weak link, defined by a hopping $t_0 \neq t$, the local particle number n_{loc} becomes inhomogeneous. We calculate the local compressibility on either side of the link defect $\kappa_{\text{loc}} = \partial n_{\text{loc}} / \partial \mu$ by differentiating it with respect to the global chemical potential μ .

For a positive link defect, i.e., t_0 has the same sign as t , we find that the peaks in the local compressibility are weakened at the transition point (Fig. 7 (a)). In the limit $t_0 = 0$ the wire is cut, the singularity in κ_{loc} is completely suppressed, though the compressibility remains finite. We also consider the case of a link with negative

hopping parameter i.e. $t_0 = -t$. Such a negative link can be produced by a local π -junction. The behavior of κ_{loc} as a function of μ is remarkably different from the positive defect. In the topological phase a sharp peak appears in the local compressibility measured on the either side of the link (Fig. 7 (b)) at a particular value of μ_0 ; for the chosen parameters, $\mu_0 = 2t$. This is due to the formation of a zero-energy bound state (Fig. 7 (c)) at μ_0 . It is important to note that this zero-energy bound state is formed only in the topological phase. At the same time, it does *not* correspond to a Majorana mode based on the structure and symmetries of the corresponding eigenfunctions (see Supplement for more details). For $\mu \neq \mu_0$ the bound state moves away from zero energy and no longer contributes to the singularity in the compressibility.

In contrast, for the Kitaev chain or for the realistic

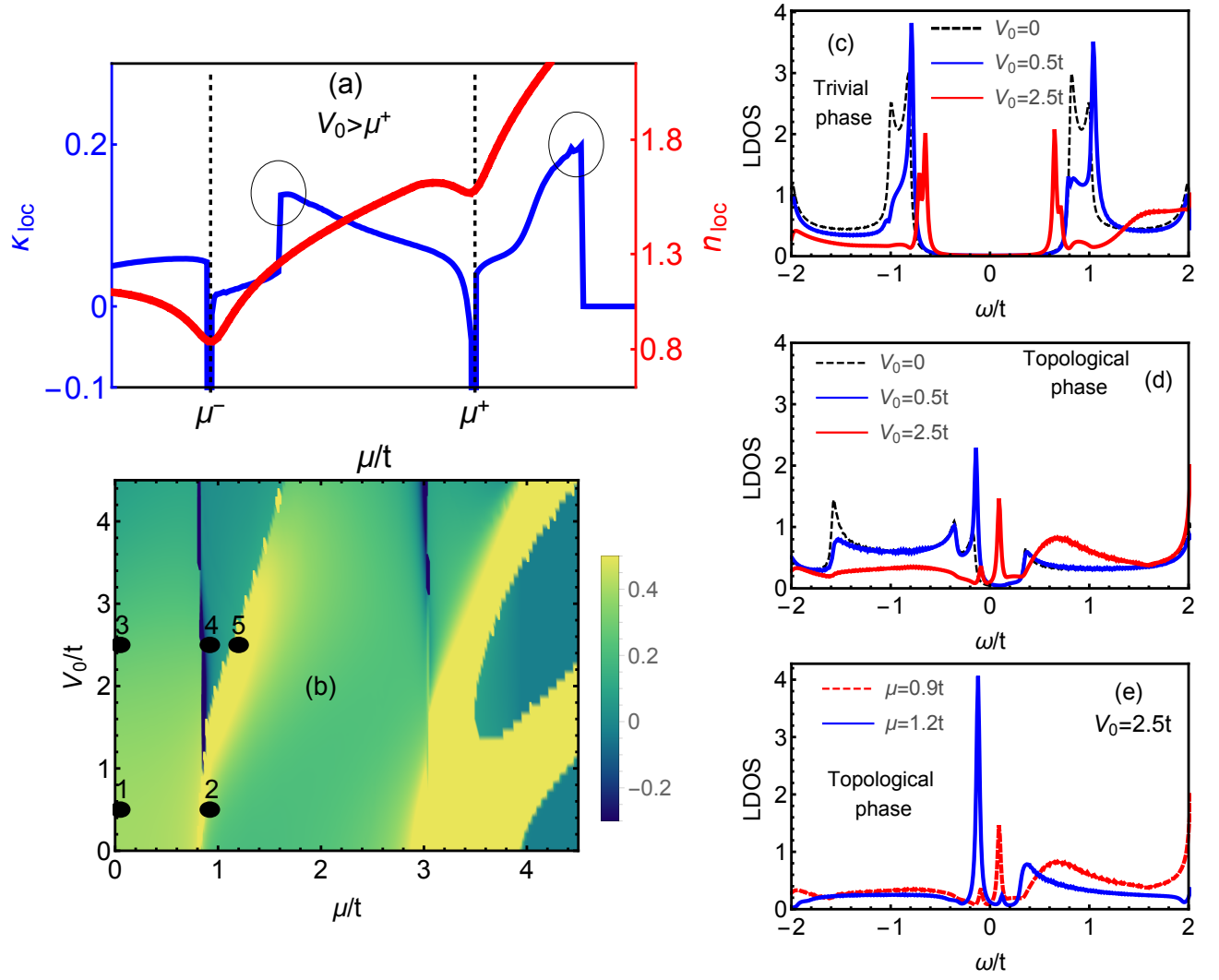


FIG. 8. (Color online). (a) The local particle density n_{loc} and κ_{loc} for a local potential defect $V_0 > \mu^+$. Close to the topological phase transitions $\mu = \mu^\pm$, κ_{loc} becomes negative. In addition, extra peaks (shown by circles) appear in the topological and trivial phases. (b) Density plot of κ_{loc} in the $\mu/t - V_0/t$ plane. (c,d,e) Local density of states for various values of V_0 and μ . (c) shows how an in-gap state appears in the presence of an on-site impurity in the trivial phase ($\mu = 0 < \mu^-$) with s and p wave parings. (d) shows how a non-trivial bound state forms in the topological phase close to the topological phase transition at $\mu = 0.9t > \mu^-$ as impurity strength V_0 increases. The bound state starts to be formed when $V_0 > \mu^-$. (e) The bound state in the topological phase for $\mu = 1.2t$.

model at μ^- , the zero energy modes are indeed Majorana modes.

When are these zero energy modes Majorana modes or simply Andreev bound states? In order to get some insight about these modes we test the corresponding eigenfunctions $u_\sigma(i)$ and $v_\sigma(i)$. If the eigenstates satisfy the symmetry conditions $u_\sigma(i) = v_\sigma^*(i)$ or $u_\sigma(i) = -v_\sigma^*(i)$ it is a Majorana mode otherwise it is an ABS fine-tuned to be at zero energy.

C. Local potential

In the presence of an on-site impurity V_0 , there are several interesting features in the behavior of the local particle density and compressibility as shown in the density plot in Fig. 8 (b).

1. Negative local compressibility

A repulsive potential $V_0 \gtrsim \mu^-$ can have a non-trivial effect on the local density and compressibility. The local particle density is found to *decrease* around the topological phase transition at $\mu = \mu^-$ even as μ increases.

Correspondingly, the local compressibility κ_{loc} becomes negative and shows a dip at the transition. For impurity strength somewhat larger than $V_0 \gtrsim \mu^+$, in addition to the dip at $\mu = \mu^-$, a second dip appears at $\mu = \mu^+$ where also the local compressibility κ_{loc} becomes negative (Fig. 8 (a)). The plot for the particle density shown here is schematic for clarity, the actual data with more details can be found in the supplementary information. The reason for the decrease of the local density and the corresponding negative local compressibility is tied to the formation of an ABS above zero energy that starts to form close to the topological phase transitions.

2. Bound states

As seen in Fig. 8 (c), In the presence of an on-site impurity, the peaks at the gap edge are suppressed and the gap size is reduced. This can be understood from the fact that the trivial phase has both s and p -wave pairing, and disorder affects the p -wave component more drastically than the s -wave component; however the spectrum remains gapped. In the topological phase where the system is effectively a “spinless” unconventional (p -wave) superconductor, a bound state is formed due to the sign change of the order parameter in this unconventional superconductor.

Figure 8 (d) shows how the zero-energy bound state starts to form when $V_0 \gtrsim \mu^-$. For a fixed V_0 as μ increases, the bound state becomes sharper and moves to zero energy. At this point the zero-energy bound state is detectable as an additional feature shown by a circle in κ_{loc} (Fig. 8 (a)). With further increase of μ the ABS moves below the chemical potential (Fig. 8 (e)). Similarly, a zero-energy ABS forms also in the trivial p -wave phase for the impurity strength $V_0 > \mu^+$.

For a negative impurity potential, the ABS forms below the Fermi level and more states shift below the Fermi energy to enhance the local density for all μ . In contrast to the scenario of the positive impurity potential, the

ABS does contribute to the local particle density for a negative impurity. As the result, the local particle density starts to increase as μ decreases, until a sharp ABS is formed. This once again causes the local compressibility to become negative around the topological phase transition.

VI. CONCLUSIONS

Our theoretical proposals based on the compressibility, in conjunction with scanning tunneling spectroscopy, are powerful diagnostics for detecting topological phase transitions in 1D spin-orbit coupled superconductors. Specifically in the presence of local defects, the local compressibility can be measured using single-electron transistor (SET) spectroscopies²⁵. Ref. 25 has in fact used the SET in a different context to measure the inverse compressibility locally on a graphene sample as a function of the back-gate voltage or carrier density. We expect the same technique can be applied to the spin-orbit coupled nanowires - superconductor devices to detect the topological phase transition guided by our predictions.

Some of the most promising directions to experimentally investigate are: (a) the sharp peak in the compressibility at the topological phase transition tuned by the Zeeman field in the clean wire, and, (b) the negative compressibility induced by the on-site impurity in the topological phase. In general it will be useful to see the interplay between local scanning and local compressibility spectroscopies for giving insights into single particle and collective modes^{26,27}.

ACKNOWLEDGEMENTS

DN and NT were supported by the NSF under Grant No. NSF-DMR1309461.

-
- ¹ C. Nayak, S. H. Simon, A. Stern, M. Freedman, and S. D. Sarma, Rev. Mod. Phys. **80**, 1083 (2008).
 - ² F. Wilczek, Nat. Phys. **5**, 614 (2009).
 - ³ A. Kitaev, Ann. Phys. **303**, 2 (2003).
 - ⁴ G. Moore and N. Read, Nucl. Phys. B **360**, 362 (1991).
 - ⁵ J. Alicea, Rep. Prog. Phys. **75**, 076501 (2012).
 - ⁶ L. Fu and C. L. Kane, Phys. Rev. Lett. **100**, 096407 (2008).
 - ⁷ J. Linder, Y. Tanaka, T. Yokoyama, A. Sudbø, and N. Nagaosa, Phys. Rev. Lett. **104**, 067001 (2010).
 - ⁸ N. Read and D. Green, Phys. Rev. B **61**, 10267 (2000).
 - ⁹ J. D. Sau, R. M. Lutchyn, S. Tewari, and S. D. Sarma, Phys. Rev. Lett. **104**, 040502 (2010).
 - ¹⁰ J. Alicea, Phys. Rev. B **81**, 125318 (2010).
 - ¹¹ M. Duckheim and P. W. Brouwer, Phys. Rev. B **83**, 054513 (2011).
 - ¹² S. B. Chung, H.-J. Zhang, X.-L. Qi, and S.-C. Zhang, Phys. Rev. B **84**, 060510(R) (2011).
 - ¹³ A. C. Potter and P. A. Lee, Phys. Rev. B (2012).
 - ¹⁴ A. Kitaev, Phys. Usp. **44**, 131 (2001).
 - ¹⁵ R. M. Lutchyn, J. D. Sau, and S. D. Sarma, Phys. Rev. Lett. **105**, 077001 (2010).
 - ¹⁶ V. Mourik, K. Zuo, S. M. Frolov, S. R. Plissard, E. P. A. M. Bakkers, and L. P. Kouwenhoven, Science **336**, 1003 (2012).
 - ¹⁷ K. Sengupta, I. Žutić, H.-J. Kwon, V. M. Yakovenko, and S. D. Sarma, Phys. Rev. B **63**, 144531 (2001).
 - ¹⁸ H.-J. Kwon, V. M. Yakovenko, and K. Sengupta, Low Temp. Phys. **30**, 613 (2004).
 - ¹⁹ L. P. Rokhinson, X. Liu, and J. K. Furdyna, Nat. Phys. **8**, 795 (2012).

- ²⁰ S. Nadj-Perge, I. K. Drozdov, J. Li, H. Chen, S. Jeon, J. Seo, A. H. MacDonald, B. A. Bernevig, and A. Yazdani, *Science* **346**, 602 (2014).
- ²¹ S. Sasaki, S. D. Franceschi, J. M. Elzerman, W. G. van der Wiel, M. Eto, S. Tarucha, and L. P. Kouwenhoven, *Nature* **405**, 764 (2000).
- ²² M. Zareyan, W. Belzig, and Y. V. Nazarov, *Phys. Rev. B* **65**, 184505 (2002).
- ²³ J. D. Sau and E. Demler, *Phys. Rev. B* **88**, 205402 (2013).
- ²⁴ C. Qu, M. Gong, and C. Zhang, *Phys. Rev. A* **89**, 053618 (2014).
- ²⁵ J. Martin, N. Akerman, G. Ulbricht, T. Lohmann, J. H. Smet, K. von Klitzing, and A. Yacoby, *Nat. Phys.* **4**, 144 (2008).
- ²⁶ C.-H. Lin, J. D. Sau, and S. D. Sarma, *Phys. Rev. B* **86**, 224511 (2012).
- ²⁷ G. Ben-Shach, A. Haim, I. Appelbaum, Y. Oreg, A. Yacoby, and B. I. Halperin, *Phys. Rev. B* **91**, 045403 (2015).